Experimental Assessment of Green Waste HTC Pellets

Garcia Lovella, Yaniel; Goel, Abhishek; Garin, Louis; Blondeau, Julien; Bram, Svend

Published in:
Energies

DOI:
10.3390/en17246474

Publication date:
2024

Document Version
Publisher's PDF, also known as Version of record

energies

MDPI

Article

Experimental Assessment of Green Waste HTC Pellets: Kinetics, Efficiency and Emissions †

Yaniel Garcia Lovella [1,2,3,4,*], Abhishek Goel [1,3,4], Louis Garin [5], Julien Blondeau [1,3,4] and Svend Bram [1,3,4]

[1] Thermo and Fluid Dynamics (FLOW), Vrije Universiteit Brussel (VUB), 1050 Brussels, Belgium; abhishek.goel@vub.be (A.G.); julien.blondeau@vub.be (J.B.); svend.bram@vub.be (S.B.)
[2] Center for Energy and Environmental Technology Assessment (CEETA), Universidad Central "Marta Abreu" de Las Villas (UCLV), Santa Clara 54830, Cuba
[3] Brussels Institute for Thermal-Fluid Systems and Clean Energy (BRITE), Vrije Universiteit Brussel (VUB), 1050 Brussels, Belgium
[4] Brussels Institute for Thermal-Fluid Systems and Clean Energy (BRITE), Belgium and Université Libre de Bruxelles (ULB), 1050 Brussels, Belgium
[5] Nanomaterials Chemistry Research Unit, Université de Namur (UNamur), 5000 Namur, Belgium; louis.garin@unamur.be
* Correspondence: yaniel.garcia.lovella@vub.be
† This paper is an extended version of our paper published in the 36th International Conference on Efficiency, Cost, Optimization, Simulation and Environmental Impact of Energy Systems (ECOS 2023), Las Palmas, Spain, 25–30 June 2023; pp. 965–976.

Abstract: The combustion of renewable solid fuels, such as biomass, is a reliable option for heat and power production. The availability of biomass resources within urban areas, such as tree leaves, small branches, grass, and other green city waste, creates an opportunity to valorize such resources. The energy densification of such resources using hydrothermal carbonization (HTC) and pelletization of the carbonized material could create a new generation of domestic boiler biofuel. However, combustion efficiency and emission assessments should be carried out for HTC pellets. The primary objective of this study is to assess HTC pellets, provided by a waste upgrade company, in terms of kinetics, combustion efficiency, and emissions, taking as reference base ENplus A1 certified softwood pellets. Therefore, thermogravimetric analysis and combustion tests were conducted for both fuels to achieve this. It was observed that a third peak of the burning rate during the solid carbon oxidation of HTC pellets indicated a high activation energy. Combustion tests showed a 7% increase in boiler efficiency for HTC pellets compared to softwood pellets. However, higher particulate matter (PM), NO_x, and CO emissions were recorded during the HTC pellets test. The results suggest that optimizing the air/fuel ratio could further improve the performance of HTC pellets in domestic boilers.

Keywords: green waste HTC pellets; softwood pellets; kinetics analysis; boiler efficiency; PM; gaseous emissions

Citation: Garcia Lovella, Y.; Goel, A.; Garin, L.; Blondeau, J.; Bram, S. Experimental Assessment of Green Waste HTC Pellets: Kinetics, Efficiency and Emissions. *Energies* **2024**, *17*, 6474. https://doi.org/10.3390/en17246474

Academic Editor: Dimitrios Sidiras

Received: 26 September 2024
Revised: 5 December 2024
Accepted: 12 December 2024
Published: 23 December 2024

1. Introduction

Biomass resources from agriculture wastes, grass, leaves, sludge from anaerobic digestion, and urban green wastes have great potential as energy resources. However, biomass resources with low energy density, high moisture content, and high alkali/alkaline earth content are challenging for direct combustion in conventional boilers [1]. Biomass pre-treatment and raw biomass upgrade into better-quality biofuels have a substantial potential to increase the feasibility of their use for heat and power generation [2,3]. Several studies have been conducted on the pre-treatment of agricultural and food waste using hydrothermal carbonization (HTC), as the work presented by Kassim et al. [4], De Francesco [5] and Balmuk et al. [6]. The main research focus has been studying the operational parameters

of the HTC process as a pretreatment method and their impact on the quality of the fuel obtained.

The HTC-pellets production at an industrial scale is not yet a feasible alternative big enough to power big power plants, considering logistic issues and suitable organic raw material availability [7]. On the other hand, HTC-pellets applications, such as small boilers for heating purposes in the residential sector, emerge as a promising opportunity to valorize low-quality organic wastes. Nevertheless, the final use of such solid fuels brings some attention related to the emissions issues, particularly concerning nitrogen oxides (NO_x) and particulate matter emissions [8,9]. Only a small group of authors, e.g., Lasek et al. [10] and Murillo et al. [11], have focused on assessing the HTC fuels and the combustion properties of the obtained hydrochar under more realistic conditions relevant to the final use of the HTC fuel, especially for small heating purposes. Therefore, the goal of the present research is to carry out a study of HTC pellets in terms of thermal and emissions performances by comparing laboratory experiment results and pilot test results against the results obtained for high-quality ENplus A1-certified softwood pellets. The main contribution or novelty of the results presented in this work lies in the combustion and emissions study of a promising biofuel for household heating applications. Additionally, the combination of laboratory kinetic experiments with pilot combustion tests constitutes a novel approach to asses such biofuel for practical applications, using the kinetic data obtained for applied purposes rather than for basic research.

2. Background

Over the last five years, a growing interest has been in obtaining carbonized fuels from low-quality biomass resources, such as green city waste and agricultural residues. It turns out that the HTC process is a viable alternative to valorize low-quality residues, obtaining a high-quality biofuel in terms of energy density and durability [12]. Table 1 shows some studies carried out in the last five years regarding producing and evaluating carbonized materials and HTC pellets. The studies compiled in Table 1 suggest a considerable effort in optimizing the HTC parameters and their impact on the quality of carbonized materials. Wu et al. have conducted an extensive literature review on HTC of food waste for sustainable biofuel production. The authors discussed the state of the proposed and actual applications of the obtained carbonized material (hydrochar). They attribute the current gap between progress in the hydrothermal carbonization (HTC) field for producing hydrochar and its practical applications to several factors: the lack of coupling technologies between hydrochar production and the power generation industry, the low standardization of the HTC process, the need for developing continuous industrial HTC reactors, and the absence of an optimized supply chain between food waste generation, hydrochar production, and their final application to consumers [13]. The arguments presented by the authors are economically interconnected. However, studies conducted in HTC mainly focus on the HTC process parameters, with practical aspects related to the final application barely addressed.

Only three surveyed studies (Table 1) specifically addressed the final application of the obtained biofuel. Murillo et al. evaluated the final application of HTC pellets obtained from oat and husk sawdust blends for domestic pellet stoves. The authors optimized HTC parameters to maximize char yield and heating value. They assessed the hydrochar pellets using gaseous emissions measurements, highlighting an increase in NO_x for HTC-treated biofuel compared to raw fuels. PM emissions were gravimetrically measured based on the particle mass captured in two quartz microfiber filters. The authors observed a considerable reduction in PM emissions compared to sawdust and commercial wood pellets [11]. However, the study was limited to HTC pellets with less than one wt.% of ash content on a dry basis. Thermogravimetric Analysis (TGA) of hydrochar pellets was not conducted, which could provide insights into char oxidation kinetics and reactivity. Additionally, with the experimental setup used, it was not feasible to further characterize PM emissions in terms of particle size distribution.

Table 1. The aspects addressed in studies found over the last five years regarding HTC-treated biomass resources.

Years	Authors	HTC Parameters	TGA [a]	F. A. [b]	G. E. M. [c]	P M [d]	Main Goal	Main Contribution
2019	Zhu et al. [14]	X	X	-	-	-	To investigate the influence of HTC parameters on the physical and chemical properties of cotton stalk hydrochar, its binderless palletization, and its combustion properties using TGA.	Considerable insights were obtained regarding the main transformation mechanisms during HTC pre-treatments and their impact on energy consumption for palletization and biofuel reactivity.
2020	Liang et al. [15]	X	X	-	-	-	To study the effects of hydrothermal treatment parameters on relevant combustion properties, mainly using TGA, and to evaluate the influence of three binders.	A combination of HTC parameters and a binder based on $CaCO_3$ was found to obtain optimal pellets from agricultural wastes.
2020	Sharma and Dubey [16]	X	X	-	-	-	To investigate the effect of HTC severity factor on yard waste regarding the fuel, mechanical, storage, transport, and combustion characteristics of the resulting hydrochar pellets	The paper demonstrates how varying HTC severity factors affect municipal yard waste hydrochar pellets, highlighting improved combustion properties and binder-free palletization feasibility.
2021	Moreira et al. [17]	X	X	-	-	-	To study reusing ash from food waste HTC as an additive for producing hydrochar pellets for solid biofuels or CO_2 adsorbents in energy systems.	The authors demonstrated the feasibility of using ash from food waste hydrothermal carbonization as an inorganic lubricant/dopant additive in pellets for both combustion and CO2 physisorption, enhancing their utility as solid biofuel.
2021	Murillo et al. [11]	X	-	X	X	X	To study the optimal obtention of sawdust and Oat husk HTC pellets and its emissions assessment for domestic pellet stoves.	The obtention of optimal HTC parameters for maximizing char yield and Heating value of hydrochar pellet and conducting a comprehensive assessment of their gaseous and PM emissions

Table 1. *Cont.*

Years	Authors	HTC Parameters	TGA [a]	F. A. [b]	G. E. M. [c]	P M [d]	Main Goal	Main Contribution
2021	Namkung et al. [18]	-	X	-	-	X	To assess the influence of different pretreatments on fuel reactivity, PM emissions, PM morphology, and chemical composition.	A factual relationship between mineral composition and PM emissions was found.
2022	Hansen et al. [19]	X	-	-	X	X	To overview the influence of changing inorganic composition in HTC-treated fuels on the risk of fine PM and NO_x emissions, as well as ash melting behavior	The effects of different hydrothermal treatment parameters on properties relevant to combustion, such as inorganic composition in the resulting fuel, were examined.
2023	Balmuk et al. [6]	X	X	-	-	-	To assess thermally treated (by pyrolysis and HTC process) olive waste from a two-phase olive mill regarding combustion performance and ash-related problems.	The authors identified optimal thermal pretreatment parameters for converting olive waste into solid biofuels with combustion characteristics comparable to lignite.
2023	Lasek et al. [10]	-	-	X	X	X	To assess the combustion and emissions performance of torrefied biomass 10 kW domestic boiler and in a 25-kW coal-fired boiler.	References values of boiler efficiency and emission factors for various thermally treated biomass feedstocks were obtained.
2023	Paniagua et al. [20]	X	-	-	-	-	To compare torrefied biomass quality regarding the inorganic composition of char derived from Napier grass via vapothermal carbonization (VTC) and HTC.	The authors describe the effects of HTC on the ash, potassium, chlorine, sulfur, and sodium contents of the obtained biofuel, alongside an assessment of the associated risks of corrosion, fouling, and slagging [e].
2023	Saha et al. [21]	X	X	-	-	-	To evaluate the influence of operational temperature in HTC of Shrimp shell on hydrochar properties, physicochemical attributes, and combustion characteristics, including the risk of fouling and slagging.	The optimal operational temperature for the HTC process was determined based on heating value, ignition temperature, ignition index, and a reduced possibility of hydrochar fouling tendency.

Table 1. *Cont.*

Years	Authors	HTC Parameters	TGA [a]	F. A. [b]	G. E. M. [c]	P M [d]	Main Goal	Main Contribution
2023	Wang et al. [22]	X	X	-	-	-	To study the effects of HTC temperature and holding time on the yield, composition, structure, combustion behavior, and safety of hydrochar for Blast Furnace Injection.	The suitable HTC parameters for industrial hydrochar production, aiming for Blast Furnace Injection, were identified, considering productivity and potential CO_2 emission reduction.
2023	Wu et al. [23]	X	X	-	-	-	To assess the impact of agricultural waste HTC temperatures on physicochemical properties of hydrochar, combustion characteristics, kinetic analysis, and the propensity of fouling and slagging.	The optimal agricultural waste HTC temperature was determined, considering thermal performance and the risk of fouling and slagging associated with the resulting hydrochar.
2024	Guo et al. [24]	X	X	-	X	-	To determine the impact of plastic waste and Ca-rich fungus bran co-torrefaction on the combustion characteristics and reactivity of Obtained biofuel.	The optimal share of plastic waste and Ca-rich fungus bran for co-torrefaction was determined, considering fuel reactivity and gas emissions analyzed through TGA coupled with FTIR measurements.
2024	Carvalho et al. [25]	X	X	-	-	-	To explore the influence of Eucalyptus grandis HTC temperature and H_2SO_4 catalyst on hydrochar production and evaluate the combustion behavior of the resulting biofuel.	The authors found a proper combination of HTC temperature and catalyst agent quantity to enhance hydrochar formation and thermal properties.

[a] TGA (Thermogravimetric analysis), it is used to indicate if TGA was conducted in the study; [b] F. A. (Final application), it is used to indicate if the final use of the fuel was addressed using pilot tests; [c] G. E. M. (Gaseous emissions measurements), it is used to indicate if gaseous emissions measurements were considered in the study; [d] PM, it is used to indicate if particulate matter emissions measurements were considered in the study; [e] Fouling and slagging: Fouling is the accumulation of unwanted materials, like soot or ash, on heat transfer surfaces, reducing efficiency and increasing maintenance needs. Slagging is the formation of molten or partially molten deposits on furnace surfaces, obstructing gas flow and reducing heat transfer efficiency.

Namkung et al. [18] studied the char combustion characteristics of empty fruit bunch (EFB) and palm kernel shell (PKS) through Thermogravimetric Analysis, ash deposition behavior, and particulate matter (PM) emissions using drop tube furnace (DTF) experiments. The authors burned raw, demineralized, and torrefied biomass samples. Torrefaction increased the fixed carbon of the EFB sample by about 6% and the PKS sample by 40% compared to raw samples. In general, torrefaction lowered the char conversion compared to the raw samples, while demineralization pretreatment did not affect char reactivity.

The removal of potassium (K), chlorine (Cl), and sulfur (S) through demineralization pretreatment decreased the ash deposition rate. Compared to raw samples, PM emissions were reduced by about 67% for the EFB sample and 49% for the PKS samples. However, torrefied samples exhibited higher PM emissions than raw and demineralized samples. PM emissions of the EFB sample increased by about 74% and about 96% for the PKS samples compared to raw samples [18]. The study provides strong evidence of the dependence of mineral composition on particulate matter (PM) emissions under highly controlled conditions. However, DTF tests are typically designed to simulate specific zones of a firing system physically. Combustion tests conducted in DTF facilities effectively address phenomena such as fouling and slagging in critical regions of a firing system. Nevertheless, the study of combustion behavior, as well as gaseous and PM emissions, is significantly influenced by factors beyond just a specific section of the firing system.

Similar trends were observed by Lasek et al. during combustion tests conducted in a 10 kWth pellets-fired boiler equipped with a drop-down feeding system. The authors assessed the emissions of CO, NO_x, and particulate matter (PM) from burned torrefied biomass and wood pellets. The study generally indicated higher CO, NO_x, and PM emission factors (on an energy basis, g/MJ) for torrefied biomass than for the wood pellet. The CO, NO_x, and PM emission factors of torrefied biomass were approximately 27%, 23%, and 14% higher than wood pellets. The increased CO emission factor was related to the combustion chamber design, which was optimized for fuels with lower fixed carbon content, such as wood pellets. Compared to wood pellets, a higher NO_x emission factor was associated with the high fuel-nitrogen content in torrefied biomass. On the other hand, PM emissions were linked to torrefied biomass forming a dusty cloud during the early devolatilization process [10]. The observed increase in the CO emission factor is majorly related to the higher fixed carbon content in the torrefied samples, which likely contributes to the rise in CO emissions. However, the study does not provide a detailed explanation of the mechanisms and phenomena responsible for this increase in unburned gaseous material. TGA experiments on the fuels could offer valuable insights into the late gasification stage of char during the combustion of torrefied biomass; such experiment results could help the authors identify potential countermeasures to mitigate this emissions behavior.

The literature surveyed suggests a gap between commercially available HTC pellets and the combustion parameters of existing small domestic boilers for heating purposes. The boiler efficiency and emission profiles should be used to assess HTC pellets in such boilers, initially designed for burning wood pellets. The present research proposes a combination of laboratory and pilot combustion experiments, targeting the final use of this novel and commercially available biofuel, allowing us to obtain practical insights into the possible utilization of HTC pellets for domestic heating purposes.

3. Materials and Methods

HTC pellets produced by an organic upgrade fuel company via HTC treatment of green city waste were tested and compared to softwood pellets as a reference. The kinetics were studied through TGA in a TGA/DSC 3+ device (Mettler Toledo company, Greifensee, Switzerland). The TGA experiments were conducted under an air atmosphere of 60.0 mL/min for softwood and HTC pellets.

The thermal efficiency and the environmental impact of the combustion of HTC pellets were assessed at the Vrije Universiteit Brussel biomass laboratory on a 40 kW MULTI-HEAT boiler (HS TARM company, Philadelphia, PA, USA). It is equipped with a gas-in-tube heat

exchanger with helical rods. The boiler is designed for fuels in the form of pellets and chips. It is connected to the thermal network, which is equipped with a PLC system with a Desigo CC Compact V6.0 QU1software (Siemens company Munich, Munich, Germany). It has various sensors to control and measure the flow rates and temperatures in the hydronic system and the boiler exhaust. Two combustion tests were carried out, the first using a high-quality fuel as wood pellets, which was taken as a reference for the second test using HTC pellets. In both tests, the exhaust gas composition was measured with a gas analyzer HORIBA PG-250 (Horiba, Ltd., Kyoto, Japan). The particulate matter was measured using an Electrostatic Low-Pressure Impactor, ELPI+ (Dekati Ltd., Tampere, Finland). Additionally, the flue gas temperature and circulation water temperatures were measured. Also, the fuel hopper was continuously weighed to measure the fuel consumption rate. The material and methods described in this work, as well as the results shown, it is an extended version of the work presented in [26].

3.1. Fuel Laboratory Characterization

Table 2 summarizes the relevant properties of physicochemical characterization of the fuels burned during the TGA experiments and the combustion tests. The laboratory characterization of the softwood pellets was taken from the work of [27]. Density analysis was carried out following the guidelines provided by standard ISO 17828 [28]. The moisture content, ash content, and volatile matter content analyses were conducted following the standards ISO 18134 [29], ISO 18122 [30], and ISO 18123 [31], respectively. The fixed carbon content was obtained by difference. The calorimetry analysis was conducted according to the standard ISO 18125 [32]. The carbon, hydrogen, and nitrogen content analyses were obtained following the standard ISO 16948 [33]. The oxygen content was computed by difference. The sulfur and chlorine content analyses were conducted following the standard ISO 16994 [34].

Table 2. Physicochemical characterization of the analyzed fuels. Source: data adapted from [27,35,36].

Properties	Units	Softwood Pellets	HTC Pellets
bulk density	kg/m^3	≥630	696
lower heating value (LHV) [a]	MJ/kg, db	≥18.8 [a]	23.12
higher heating value (HHV) [a]	MJ/kg, db	≥20.2 [a]	24.36
moisture content	wt.%, ar	<8	5.8
volatile matter	wt.%, daf	(77.7)	69.1
fixed carbon	wt.%, daf	(22.3)	30.9
ash content	wt.%, ar	(0.3)	11.0
carbon (C)	wt.%, db	(52.2)	57.9
hydrogen (H)	wt.%, db	(5.9)	5.7
nitrogen (N)	wt.%, db	≤0.3	1.26
oxygen (O)	wt.%, db	(39.1)	23.3
sulfur (S)	wt.%, db	≤0.04	0.137
chlorine	wt.%, db	≤0.02	0.092

wt.%: percentage on weight basis; ar: as received; db: dry basis; daf: dry basis and ash free. The values in brackets are the median of similar softwood pellets taken for the original author [27] from the public Phyllis2 database. [a] The heating values were computed by the original author [27] using the Boie model [37].

It can be noticed that HTC pellets have a higher lower heating value (LHV) than softwood pellets, about 18% higher. The higher LHV of the HTC pellet is reflected in the higher fixed carbon content, which is expected in a highly carbonized product obtained from the HTC process. Elemental composition shows low chlorine amounts in the tested HTC and softwood pellets. However, the chlorine quantity in the HTC pellets is about five times higher than in the softwood pellets, which might represent a long-term corrosion risk for the firing system. Other important features of the HTC pellets are the higher nitrogen and ash content than softwood pellets, considering their potential contribution to NO_x and PM emissions.

3.2. Experimental Setup for Emissions Assessment

PM and exhaust gas composition measurements were simultaneously carried out, as Figure 1 shows. The exhaust gas composition was measured on a volumetric and dry basis.

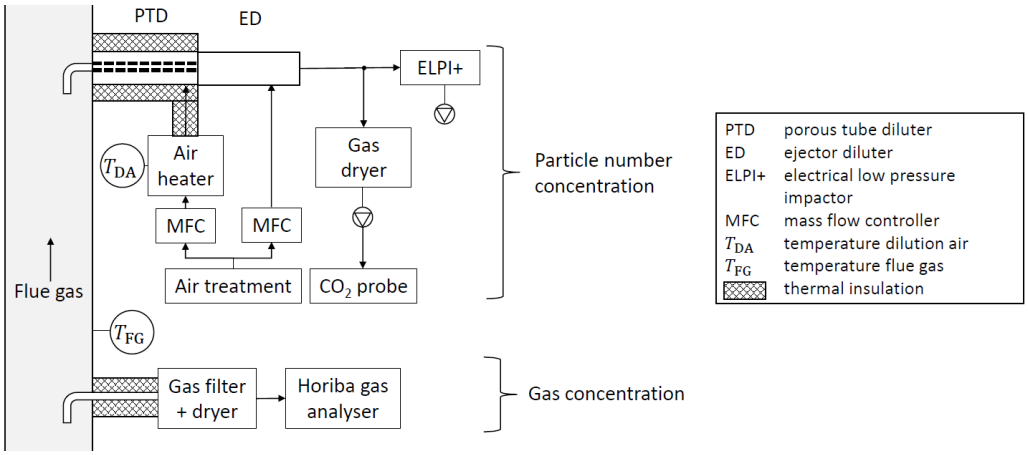

Figure 1. Scheme of equipment for measuring particulate and gaseous emissions. Source: taken from [27] and modified by the authors.

PM measurement was carried out by diluting the combustion products with air using a two-stage dilution system to control parameters like temperature, humidity, and particulate concentration according to the specifications of the measuring device. This configuration increases the reliability of the ELPI+. Additionally, it minimizes the probability of modifications in the PM distribution due to aerosol chemistry during the measurement process, as suggested by the work of Cornette [38].

3.3. Indexes for Combustion Characterization and Kinetics

The ignition and burnout characteristics of a fuel are commonly related to the ignition temperature (T_i) and the burnout temperatures (T_b). Ignition temperatures are estimated graphically (Tangent Method), and the first peak point of the TG first-derivate (DTA) is used as an intersection point with the TG curve, as described in [39,40].

The fuel thermal degradation is expressed as Equation (1) shows, with W_i being the initial mass fraction of the sample, W the remaining mass fraction of the sample, and W_f the final mass fraction of the sample

$$\alpha = \frac{W_i - W}{W_i - W_f}, \quad (1)$$

The burnout temperature can be estimated via the "Conversion Method", suggested by [41]. The method uses a simple criterion for selecting the burnout temperature, which considers T_b at the point where the fuel reaches 99% of thermal degradation $(\alpha = 0.99)$. The tangent method may be used. Nevertheless, authors such as Liu et al. suggest that in cases where the air is used as a carrier gas during TGA, two distinct peaks appear; then the tangent method should be used for the estimation of burnout temperature by using the second DTG peak as intersection point instead of the first DTG peak [39].

Combustion characteristics of biomass fuels can be assessed by the index S [42]. Equation (2) shows the formula to compute a comprehensive combustion index.

$$S = \frac{(d\alpha/dt)_{max} \cdot (d\alpha/dt)_{mean}}{T_i^2 \cdot T_b}, \quad (2)$$

The index considers the maximum fuel conversion rate $[(d\alpha/dt)_{max}]$ and the average value $[(d\alpha/dt)_{mean}]$. A higher comprehensive combustion index represents a higher fuel

reactivity, which results in better fuel combustion performance [43]. In biomass combustion, pyrolysis is one of the most difficult stages to account for accurately. Nevertheless, some general conversion routes can be assumed: biomass → char + volatiles + gases. Depending on the pyrolysis regime, the amount of products can vary [44,45]. This work studies the combustion reaction kinetics of softwood and HTC pellets using data obtained from TGA experiments. There are several methods available in the literature for modeling the combustion reaction kinetics, such as the Kissinger-Akahira-Sunose (KAS) method [46,47], Ozawa-Flynn-Wall method (OSF) [48,49] or Coats–Redfern method [50]. The present study selected the Coats–Redfern method, considering its simplicity and the possibility of estimating the activation energy and the pre-exponential factor with a minimum of TGA experiments.

3.4. Efficiency and Emission Factor Calculation

Besides the theoretical study of the combustion reaction kinetics of the HTC pellets, the final use application of this HTC fuel was also assessed experimentally. In the present study, the boiler and combustion efficiency is calculated from the parameters measured during the combustion tests. In this case, using a more practical approach, Equation (3) shows the efficiency model of a boiler using the direct method.

$$\eta_B = \frac{\dot{Q}_L}{\dot{Q}_F}, \tag{3}$$

$\dot{Q}_L$ represents the thermal power transferred from the fuel to the feeding water of the boiler. As the water vapor in the exhaust gases is not condensed, the LHV is used to compute the thermal power from the fuel $\dot{Q}_F$. The indirect method for computing the efficiency in the boiler is a more interesting option, considering the possibility of identifying the critical point related to all the effects that cause a reduction in boiler efficiency. However, calculating boiler and combustion efficiency using the indirect method requires a representative sampling of bottom and fly ashes in the boiler. In a small fixed-bed boiler, at least 24 h of operation will be necessary to get an expected amount of bottom ash, completing one cycle of ash out of bed. Nevertheless, Good and Nussbaumer have proposed a simplified method for computing the combustion efficiency of biomass boilers [51,52]. The method has been successfully applied if CO ≤ 0.5 vol%, CO_2 ≥ 5 vol%, and exhaust gas temperatures below 400 °C [53].

$$\eta_C = 100 - L_{th} - L_{ch}, \tag{4}$$

Equation (4) relates the combustion efficiency to two parameters: the thermal (L_{th}) and chemical losses (L_{ch}).

$$L_{th} = \frac{\left(T_{fg} - T_A\right)\left\{1.39 + \frac{122}{CO_2+CO} + 0.02{\cdot}u\right\}}{\frac{LHV}{100} - 0.2442{\cdot}u}, \tag{5}$$

$$L_{ch} = \frac{CO}{CO_2 + CO}\frac{11800}{\frac{LHV}{100} - 0.2442{\cdot}u}, \tag{6}$$

T_{fg} and T_A stand for the temperature of the exhaust gases and atmosphere. CO and CO_2 are the carbon monoxide and carbon dioxide volume fractions measured on a dry basis. u represents the fuel moisture expressed in percentage. Additionally, by expressing the energy balance on the boiler, some approximation of the losses regarding unburned carbon on the bottom and fly ash can be made. Equation (7) represents the energy balance for a steady-state operation of the boiler

$$\dot{E}_{in} = \dot{E}_{out} \tag{7}$$

Then, identifying all energy flows involved in the process, as Equation (8) shows, an estimation of energy losses regarding unburned fuel $\left(\dot{Q}_{\mathrm{UBF}}\right)$ can be computed as

$$\dot{Q}_{\mathrm{F}} = \dot{Q}_{\mathrm{L}} + \dot{Q}_{\mathrm{FG}} + \dot{Q}_{\mathrm{UBF}} + \dot{Q}_{\mathrm{RC}}, \tag{8}$$

The values of the thermal load and thermal power from the fuel are known values from the direct method mentioned earlier. The losses by radiation and convection $\left(\dot{Q}_{\mathrm{RC}}\right)$ of the boiler can be neglected. However, Lyubov et al. found that for industrial hot-water boilers, the losses by convection and radiation to the environment are less than 0.5% of the thermal power supplied by the fuel to the boiler furnace [54]. Then, with the value of losses by unburned fuel, Equation (9) can compute the combustion efficiency, which is based on the total power from the fuel and the power not used by unburned fuel.

$$\eta_{\mathrm{C}} = \left(1 - \frac{\dot{Q}_{\mathrm{UBF}}}{\dot{Q}_{\mathrm{F}}}\right), \tag{9}$$

The emission factors (EF) are computed on an energy density basis, allowing us to compare emission factors from different combustion tests without considering differences in oxygen concentrations.

$$\mathrm{EF_e} = \frac{\dot{m}_{\mathrm{i}}/\Delta t}{\left(\dot{m}_{\mathrm{f}}/\Delta t\right)\cdot \mathrm{LHV}}, \tag{10}$$

In Equation (10), m_{i} represent the mass of each pollutant emitted during the considered time window (Δt). The emission factors for particle number of $PM_{2.5}$ and PM_{10} are computed according to Equations (11) and (12).

$$n_{\mathrm{PM}} = y_{\mathrm{n}} \cdot \mathrm{DR}_2 \cdot \dot{V}_{\mathrm{fg,dil,dry}}, \tag{11}$$

$$\mathrm{EF_{PMx}} = \frac{n_{\mathrm{PM}}/\Delta t}{\left(\dot{\mathrm{m}}_{\mathrm{f}}/\Delta t\right)\cdot \mathrm{LHV}} \tag{12}$$

In Equation (11), y_{n} represents the particle number, DR_2 stands for dilution ratio at dilution stage two and $\dot{V}_{\mathrm{fg,dil,dry}}$ represent the volumetric flow of diluted exhaust gases at dry conditions.

4. Results and Discussions

4.1. Kinetic Analysis of the Fuels

In general, during TGA experiments of lignocellulose-biomass under oxidative conditions, an initial drying step can be observed (of free water, crystal water, and absorbed water), which extends from room temperature up to about 170 °C. The second step is when volatilization and combustion of volatiles start, extending from about 120 °C to about 420 °C. Then, a third step of char oxidation starts from a temperature range of about 310 °C up to about 520 °C. Finally, the burnout step appears when all remaining char is consumed, starting at about 480 °C [55,56]. The temperature range of each step of biomass combustion shown by the TGA experiments varies with the type of biomass and is also affected by the heating rate. However, the values could be taken as a reference for other biomass samples, considering that the mentioned author analyzed 12 different types of biomass using different heating rates.

Figure 2a shows the derivative thermogravimetric curve (DTG), and Figure 2b shows the TGA of softwood pellets of the same sample. The drying step extends from 25 °C up to 95 °C, followed by an almost flat zone, where a nearly constant weight loss rate (about 0.42%) is observed over a temperature range of about 100 °C. The more active drying range and the almost constant weight loss rate were grouped into step A. Step B corresponds to the release and combustion of volatiles, coming from the hemicellulose at the beginning

and cellulose at the end of this step. The highest weight loss is observed between 197 °C and 357 °C. Step C ranges from 357 °C to 500 °C, where the char coming from the lignin is oxidized. However, some authors point out that some char could also appear at the end of step B [44,57,58]. The burnout step starts at 500 °C, completely oxidizing the char. For the present analysis, two zones were studied further: Zone I (197 °C–357 °C) and Zone II (357 °C–500 °C).

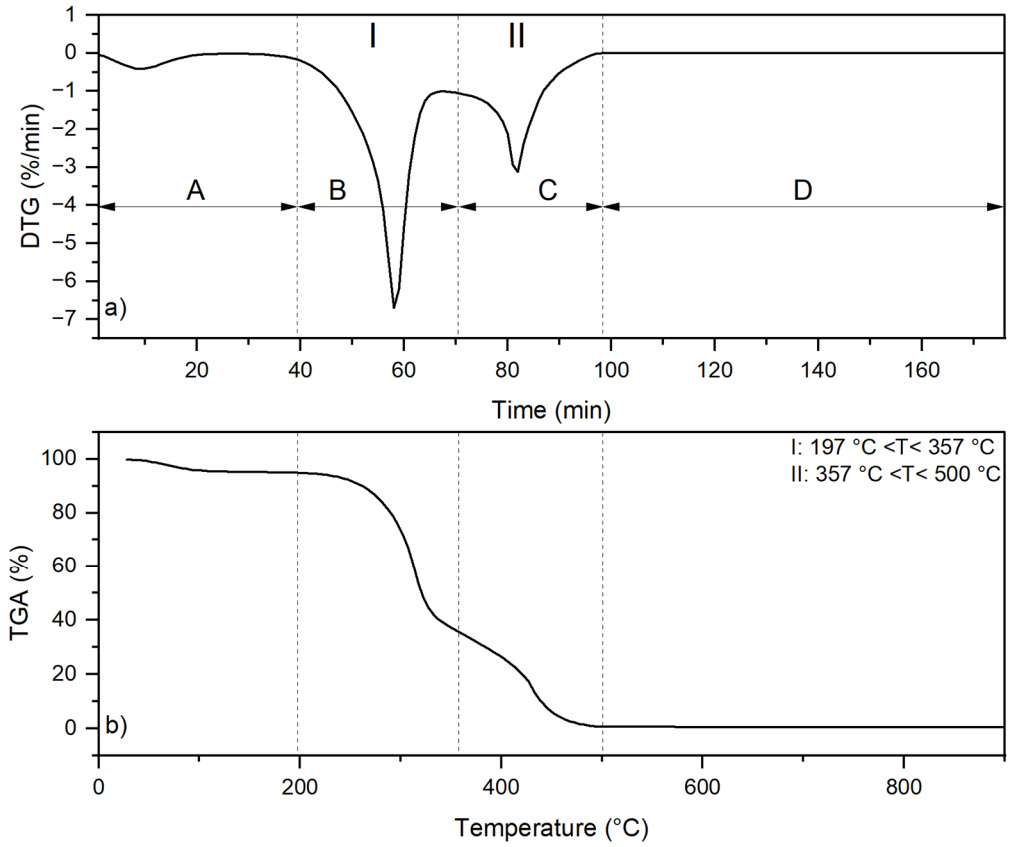

Figure 2. Thermal degradation of softwood pellets: (**a**) The derivative of thermogravimetry (DTG) analysis. (**b**) Thermogravimetry analysis (TGA).

Figure 3a shows the DTG of HTC pellets, and Figure 3b shows the corresponding TGA curve. As for the softwood pellets, four steps can be identified (A to D), but there are some differences to be noticed. Step A extends in the temperature range of about 15 °C more for HTC pellets than for softwood pellets. Additionally, two distinct peaks can be observed. The first one is from 25 °C to 117 °C, which is assumed to correspond to the evaporation of free water in the fuel. The second is from 117 °C to 212 °C, corresponding to the evaporation of the crystal water and absorbed water contained in the fuel structure. Step B extends from 212 °C to 322 °C. The temperature span for this step is 50 °C less for HTC pellets than for softwood pellets. The difference in the temperature range of step B between softwood pellets and HTC pellets may be influenced by the higher content of volatile matter in the softwood pellets compared to the HTC pellets.

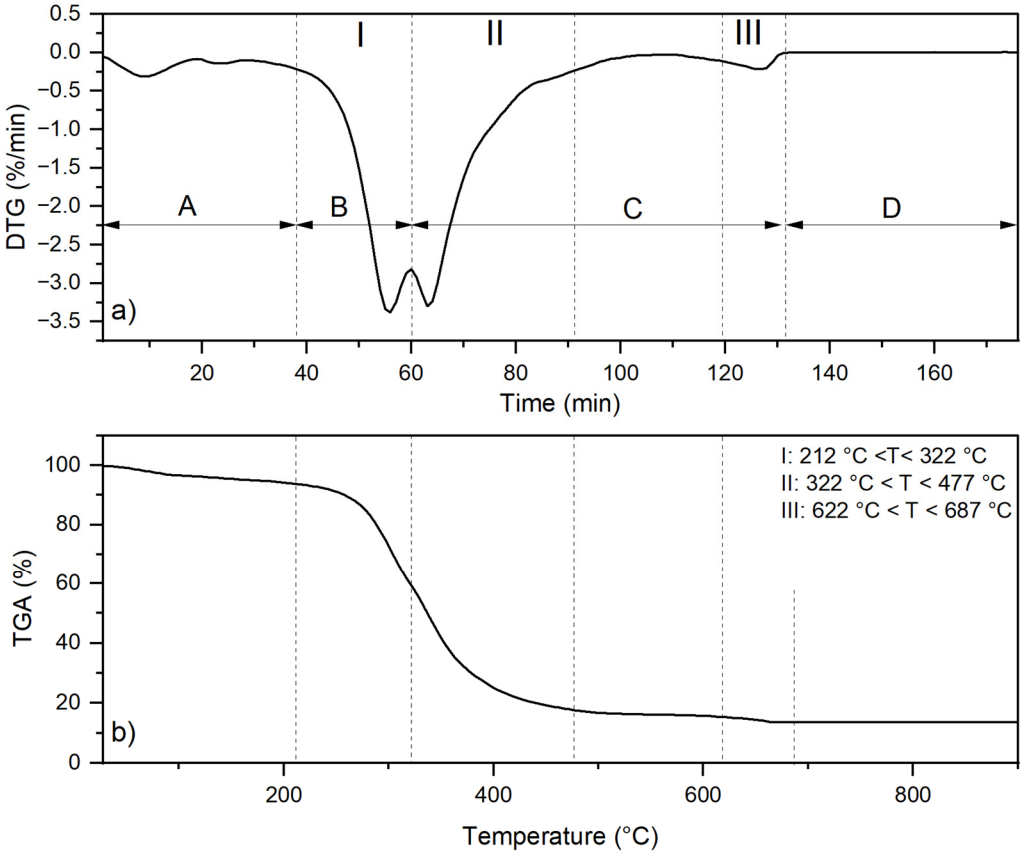

Figure 3. Thermal degradation of HTC pellets: (**a**) The derivative of thermogravimetry (DTG) analysis. (**b**) Thermogravimetry analysis (TGA).

Step C, from Figure 3a, shows a quite different shape for HTC pellets than for softwood pellets. The peak corresponding to the zone of maximum burning rate for step C is similar to the peak observed in step B. Also, the burning rate is quantitatively similar. However, step C starts at 322 °C and ends at about 477 °C. For the softwood pellets, the higher part of the fuel mass is released in step B: 59.3% versus 34.9% during step C. The opposite trend is observed for HTC pellets; 34.5% of the mass is released in step B versus 45.4% in step C. Another peculiarity of step C is a second peak; after a big peak, there is a trend in the TGA (Figure 3b) where the mass burned remains almost constant from 477 °C to 622 °C, with a weight loss of only 1.8%. But after 622 °C, the weight loss increases, making a second peak in step C. It can be noticed more clearly from the DTG curve (Figure 3a) from 622 °C to 687 °C. The peaks shown in the DTG curve of HTC pellets were defined as three zones of kinetics interest for further analysis, as pointed out in Figure 3a. In general, the smaller difference in the burning rate of the two peaks showed by the HTC pellets, compared to the bigger difference between the two peaks of steps B and C of softwood pellets, strongly suggests a less chaotic burning rate and better combustion stability for the HTC pellet.

Table 3 shows the comprehensive combustion index *S*. It clearly shows that the index is bigger by about one order of magnitude for HTC pellets than for softwood pellets. Some authors claim that a higher *S* index indicates a higher fuel reactivity and a better fuel combustion performance. The ignition temperature of the two fuels is quite similar, which means that HTC pellets are as easy to ignite as softwood pellets. Nevertheless, the burnout temperature obtained from the tangent method is smaller for HTC than for softwood pellets. Still, considering Figures 2 and 3, it can be noticed that the tangent method showed a poor physical meaning regarding burnout temperature. Using the conversion method suggested by Lu and Chen [41], the burnout temperatures of HTC pellets and softwood pellets can be estimated again, which leads to 500 °C and 687 °C for softwood pellets and HTC pellets,

respectively. The new burnout temperature allows the re-computing of a comprehensive combustion index, which in this case is for both cases in the same order but slightly better for HTC pellets.

Table 3. Characteristic combustion parameters for softwood pellets and HTC pellets.

Biomass Sample	Ignition Temperature (°C)	Burnout Temperature (°C)	Temperature at Maximum Burning Rate (°C)	Index S ($min^{-2} \cdot K^{-3}$)
softwood pellets	257	474 (500) [a]	293	1.45×10^{-10} (1.23×10^{-10}) [b]
HTC pellets	259	392 (687) [a]	301	1.45×10^{-9} (2.57×10^{-10}) [b]

[a] The value in brackets represents the estimated burnout temperature using the conversion method. [b] The value in brackets corresponds to the recomputed comprehensive combustion index based on the new burnout temperature.

Char oxidation is a multi-phase phenomenon, and between 477 °C and 722 °C, the inorganic compounds from the ashes form the bigger part of the remaining fuel mass. It can be that some small amount of char is trapped in the ashes; therefore, a higher temperature and longer time could be required for the diffusion of oxygen to reach the char and be completely depleted. This can be the reason for higher burnout temperatures; in some way, a higher temperature will enhance the porosity of the remaining particles, and as a result, oxygen diffusion to the char can be enhanced. Khoo et al. [59] observed a similar behavior during the TGA of hydrochar derived from high-ash, low-lipid microalgal biomass through hydrothermal carbonization. The authors referred to the final peak observed in the DTG curves as a passive combustion reaction zone. HTC process provokes an increase in ash content and concentration of inorganic compounds, such as magnesium (Mg) and calcium (Ca). Calcium carbonate ($CaCO_3$) and magnesium carbonate ($MgCO_3$) will further decompose in the HTC fuel during this passive combustion zone to finally release CO_2. However, the decomposition of calcium and magnesium carbonates will form calcium, magnesium monoxides, and carbon dioxide as more stable compounds depending on several factors: particle size of the carbonates, the porosity of the remaining carbon-ash matrix, temperature, residence time of intermediate species as carbon monoxide before complete oxidation and oxygen amount [60,61].

Figures 4 and 5 show the fitting curves of softwood pellets and HTC pellets for different combustion reaction stages through multiple first-order reactions.

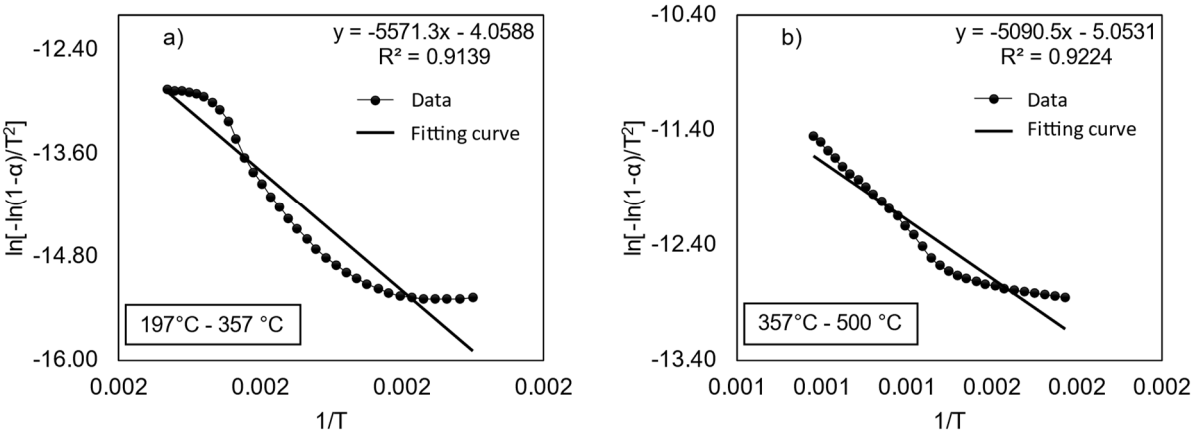

Figure 4. Fitting curve for reaction stages of softwood pellets: (**a**) temperature range from 197 °C to 357 °C and (**b**) temperature range from 357 °C to 500 °C.

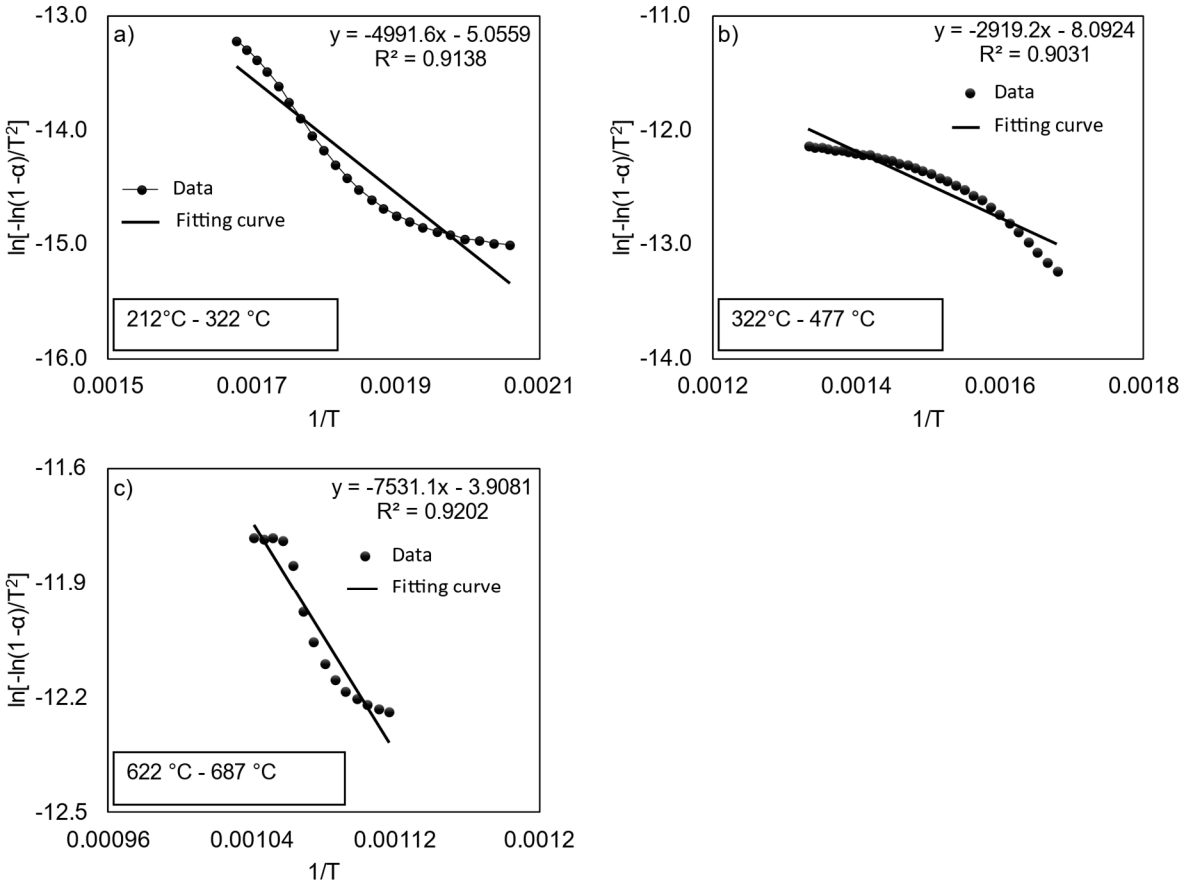

Figure 5. Fitting curve for reaction stages of HTC pellets (**a**) temperature range from 212 °C to 322 °C, (**b**) temperature range from 322 °C to 477 °C and (**c**) temperature range from 622 °C to 687 °C.

The DTG curves for softwood pellets were divided into two main reaction stages or reaction zones, in the temperature range of 197 °C to 357 °C (zone I in Figure 2a) and from 357 °C to 500 °C (zone II in Figure 2a). In both reaction zones, the correlation coefficients are higher than 0.91, which suggests that the assumption of a first-order reaction might be sufficient for first-order modeling of the pyrolysis and char oxidation processes.

The first reaction zone considers the volatilization and combustion of volatiles, and the second is the volatilization and combustion of char. The time of both reaction zones is quite the same, but zone II occurs at a lower burning rate than zone I, about 2.2 times lower than zone I. Table 3 shows the kinetic parameters for tall reaction zones, outlined in Figures 4 and 5. The required activation energy is bigger for zone I than zone II, suggesting a slower reaction rate for such zones.

Table 4 shows the kinetic parameters of softwood and HTC pellets, being the activation energy of HTC pellets in the temperature range from 622 °C to 687 °C higher than in the other two temperature ranges.

Table 4. Kinetic parameters in different temperature ranges.

Biomass Sample	Temperature Range (°C)	Activation Energy (kJ/mol)	Pre-Exponential Factor (min^{-1})
Softwood pellets	197–357	46.32	1.61×10^6
	357–500	42.32	3.98×10^6
HTC pellets	212–322	41.50	3.92×10^6
	322–477	24.27	4.77×10^7
	622–687	62.61	1.88×10^6

The TGA DTG curves for HTC pellets were divided into three main reaction zones, showing correlation coefficients above 0.90. The first reaction zone represents the volatilization and combustion of volatile matter, and the second is the volatilization and combustion of the major part of char. In this case, as a highly carbonized fuel obtained employing the HTC process, the fixed carbon is in a higher quantity than conventional lignocellulosic biomass. Therefore, burning rate peaks are quite similar. However, the activation energy of the reaction in zone II is 1.7 times smaller than the activation energy in reaction zone I. Combustion zone III can be assumed as an extension of the char volatilization of zone II, which requires the highest activation energy of all zones considered in HTC pellets. The analysis of zone II and III together, or even zone III alone, suggests that a small amount of char is the reaction rate limiting, which may represent a critical reaction zone for achieving an efficient HTC pellets combustion.

4.2. Combustion and Emissions Study in a Pilot Boiler

Figure 6 shows the difference in boiler efficiencies between the tests performed with softwood pellets and HTC pellets, which is about 7% higher for HTC pellets than for softwood pellets.

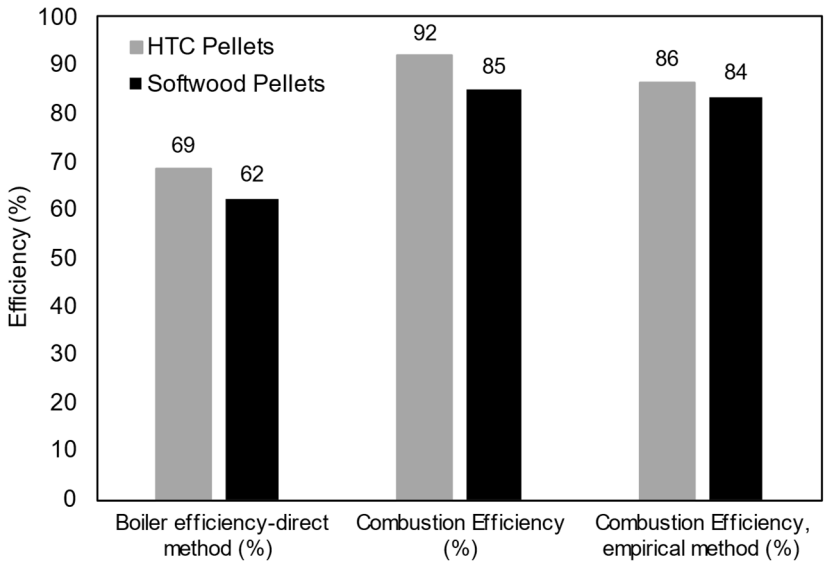

Figure 6. Boiler efficiency (direct method) and combustion efficiency (calculated from the indirect method and using the empirical method).

The indirect method for calculating the boiler efficiency showed that flue gas losses accounted for about 18% of HTC pellets and 22% of softwood pellets. The losses regarding the unburnt fuel ($\dot{Q}_{UBF}$ in Equation (8)) of HTC pellets and softwood pellets were about 8% and 15%, respectively. Visual observation at the end of the tests confirmed the values obtained for losses by unburned fuel. Figure 7 shows the bottom ash collected at the end of each test. The highly unburnt charcoal in the bottom ash of softwood pellets could suggest the need for more extended boiler operation (more than 3 h) in steady-state operation for bottom ash sampling. A complete cycle of ash removal from the boiler bed may be necessary. Nevertheless, for the HTC pellets test without a complete cycle of ash removal from the boiler bed, Figure 7a shows a higher charcoal burnout than softwood pallets (Figure 7b).

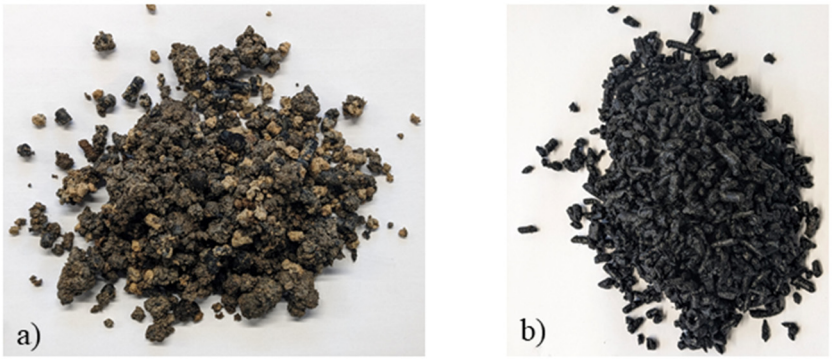

Figure 7. State of bottom ash at the end of the tests: (**a**) HTC pellets; (**b**) softwood pellets.

The temperature difference between the exhaust gases and the environment for both tested fuels is almost the same, with only a two degrees Celsius difference between each test. Still, the difference in loss regarding hot gases is primarily due to the mass flow rate. Both fuels are burned with similar air-fuel ratios (AFR): 29.3 kg_{air}/kg_{fuel} for softwood pellets and 29.5 kg_{air}/kg_{fuel} for HTC pellets. Despite the slightly higher AFR required for HTC pellets, the low energy density of softwood pellets makes it necessary to supply more fuel mass into the combustion chamber. As a result, more air is required, and more exhaust gases are produced, increasing heat losses to the atmosphere. Figure 6 shows that the combustion efficiency of HTC pellets is higher than the combustion efficiency of softwood pellets. Despite the quantitative differences shown by the methods, the results are consistent. Both methods show that HTC pellets are burned more efficiently in the used boiler under similar operational parameters.

Table 5 shows the measurements of flue gas composition for softwood and HTC pellets under measurement conditions and normalized at 10 Vol. % oxygen concentration. The normalized results indicate similar values for carbon dioxide concentration. However, the values for carbon monoxide and nitrogen oxides were considerably higher for HTC pellets than softwood pellets.

Table 5. Emissions measurements and normalized values.

Parameter	Units	Softwood Pellets		HTC Pellets	
		Average Value	Standard Deviation	Average Value	Standard Deviation
$PN_{n,\ total}$	$\#/m^3$	2.95×10^{11}	4.97×10^{10}	6.66×10^{11}	2.28×10^{10}
		Measurements at real O_2 concentration			
O_2	Vol. %	15.30	0.20	15.50	0.98
CO	ppm	8	3	166	56
CO_2	Vol. %	5.71	0.17	5.34	0.87
NO_x	ppm	35	2	96	16
		Measurements normalized at 10 Vol. % of O_2 concentration			
CO	ppm	15	7	331	88
CO_2	Vol. %	10.14	3.01	10.72	0.53
NO_x	ppm	62	18	201	64

Figure 8 shows the emission factor (EF) for the measured gaseous emissions in terms of pollutant mass per unit of energy. The combustion of softwood showed a slight increase in carbon dioxide emission factor concerning HTC pellets, 8 g/MJ more than HTC pellets.

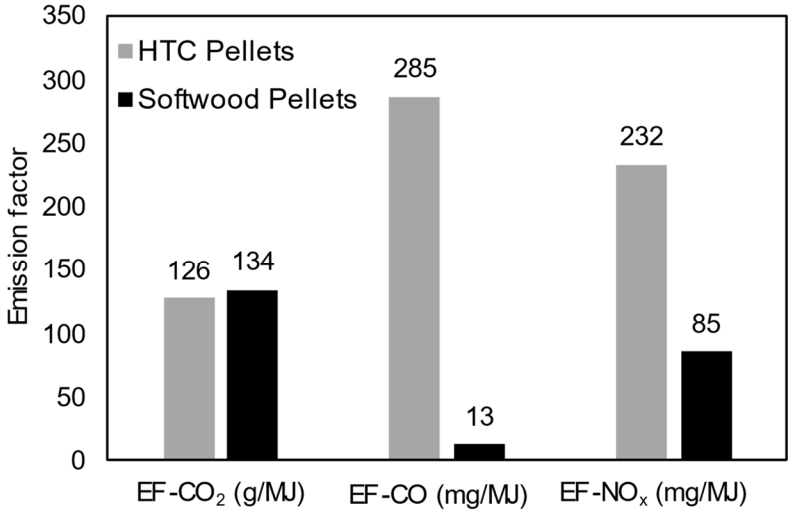

Figure 8. Emission factor for softwood and HTC pellets.

This higher emission factor for carbon dioxide could mean that softwood pellets tend to completely oxidize more carbon instead of remaining in the form of carbon monoxide. The peak of the char gasification for softwood pellets occurs at a higher temperature than for HTC pellets (416 °C for Softwood pellets and 336 °C for HTC pellets. The volatiles released during this stage found better kinetic conditions for the complete oxidation of gaseous combustible material. As expected, the carbon monoxide emissions factor is higher for HTC pellets than for softwood pellets, which is related to the lower reaction rate of the kinetics in reaction zone III, as shown in Figure 3a. On the other hand, the HTC pellets have a higher fixed-carbon content with 8.6% more fixed carbon than softwood pellets. The late release of carbon monoxide as an intermediate species on the decomposition of calcium and magnesium carbonate in the ash matrix could influence the higher CO emissions factor of the HTC pellets. In general, the lower combustion efficiency showed by the softwood pellets is related to the amount of unburned char found in the bottom ash. The lower bulk density and lower LHV of softwood pellets, compared to HTC pellets, led to a higher volume of fed softwood pellets into the combustion chamber to meet similar thermal power requirements of the boiler during the tests. The fuel excess in the combustion chamber does not benefit the combustion aerodynamics and the heat transfer process in the fuel bed, lowering char gasification and oxidation under the high thermal load operation of the boiler.

The NO_x emissions during biomass combustion originate from three gas-phase reaction mechanisms: the thermal NO_x mechanism (nitrogen oxidation due to high temperatures, usually higher than 1300 °C), the prompt NO_x mechanism (reaction of CH radicals with atmospheric nitrogen in areas close to the flame front), and the fuel NO_x mechanism (oxidation of the nitrogen contained in the fuel). The thermal and prompt NO_x mechanisms are more significant in the combustion of fossil fuels, where the average temperature of the furnace could be higher than 1300 °C. Usually, the firing systems designed for biomass combustion operate at temperatures between 900 °C and 1000 °C, with peaks up to 1300 °C. Therefore, the fuel NO_x mechanism dominates nitrogen emissions during biomass combustion [62]. Other authors state that regardless of the implemented firing system, about a third of the nitrogen in solid biofuel is generally converted to nitrogen monoxide [63], which makes the nitrogen content in biomass fuels critical regarding NO_x emission. EF-NO_x of HTC pellets shows a considerably higher value than softwood pellets, which was expected considering that elemental analysis (see Table 1) shows that nitrogen in the fuel is more than four times higher for HTC pellets than softwood pellets. The NO_x emissions associated with the nitrogen in the fuel (fuel-N) are described by complex homogeneous and heterogeneous reaction pathways of NO formation and NO reduction. Fuel-N is usually divided into two parts: volatile nitrogen (volatile-N) and the remaining nitrogen in the char matrix (char-N).

The first part is released with the volatiles during pyrolysis, which breaks down from tars to NH radicals to form nitrogen monoxide. The second part of the fuel-N is retained in the char matrix, which is oxidized in oxygen-rich atmospheres. However, the initially oxidized char-N could be reduced by interacting with the porous char particles through heterogeneous or homogeneous reactions in the presence of carbon monoxide, catalyzed by calcium (Ca) and magnesium (Mg) from the ashes. Additionally, more NO and N_2O could be formed from the interaction of the char matrix with HCN and CH radicals. On the other hand, some N_2O could be transformed into elementary nitrogen in atmospheres with water vapor and carbon monoxide. Both nitrogen conversion routes contribute to the NO_x emissions. However, the amount of fuel-N distributed between volatile-N and char-N is nearly proportional to the volatile amount in the fuel, with the volatile-N contribution to NO_x formation between 70% and 90% [64–66]. On the other hand, volatile-N is more difficult to prevent from transforming into NO_x emission than char-N. The HTC pellets have a lower ratio of volatile matter to fixed carbon than softwood pellets. Nonetheless, 56% of fuel-N is converted into NO_x for HTC pellets and 27% for softwood pellets, which could indicate that the pretreatment of the row biomass has concentrated the nitrogen in the char matrix. The higher conversion percentage of fuel-N to NO_x during HTC pellets combustion could be related to the observations made by Kaivosoja et al. [67], whereas the fixed carbon content increases, nitrogen trends to bind in heterocyclic structures leading to the formation of HCN, rather than being present in the form of amines or quaternary-N structures, being formed NH_3 which is a better reductant of NO than HCN, which tends to reduce NO to N_2O rather than to N_2. The N_2O can be transformed to NO under fuel-lean conditions close to the fuel bed and at moderately low temperatures.

Figure 8 shows the emissions factor of PM up to 2.5 µm (EF-$PM_{2.5}$) for HTC pellets and softwood pellets.

The particulate matter measurements have shown that more than 99% of the emitted particles were concentrated up to 2 µm. Then, the emission factor for particulate emission was computed only for $PM_{2.5}$ (see Figure 9). The EF-PM2.5 for HTC pellets was more than twice as high as for softwood pellets. The high ash content of HTC pellets, which was more than ten times higher than that of softwood pellets, likely contributed to the elevated PM emission factor of the HTC pellets. The high fixed carbon content of the HTC pellets might contribute to the presence of unburned carbon (soot) in the flue gases, which could be the reason for the drastically higher emissions factor for $PM_{2.5}$. Figure 10 shows a clear difference in particle size distribution for softwood and HTC pellets. The 10% cumulative distribution (D10) of PM emission is up to particle diameter 0.016 µm for the softwood pellets and 0.0248 µm for the HTC pellets. The 50% cumulative distribution (D50) of PM emission is up to particle diameter 0.0406 µm for the softwood pellets and 0.0701 µm for the HTC pellets. The 90% cumulative distribution (D90) of PM emission is up to particle diameter 0.0701 µm for the softwood pellets and 0.1295 µm for the HTC pellets.

Figures 10 and 11 show that for particle diameters between 0.0091 and 0.0248 µm, the particle number for the softwood pellets was higher than for the HTC pellets. Nonetheless, in the particle diameter range of 0.0406 to 3.0169 µm, the particle number for the HTC pellets was far higher than that of the softwood pellets. It can be realized that the higher particle number count for both burned fuels is concentrated in the diameter range of 0.0091 µm to 0.43 µm.

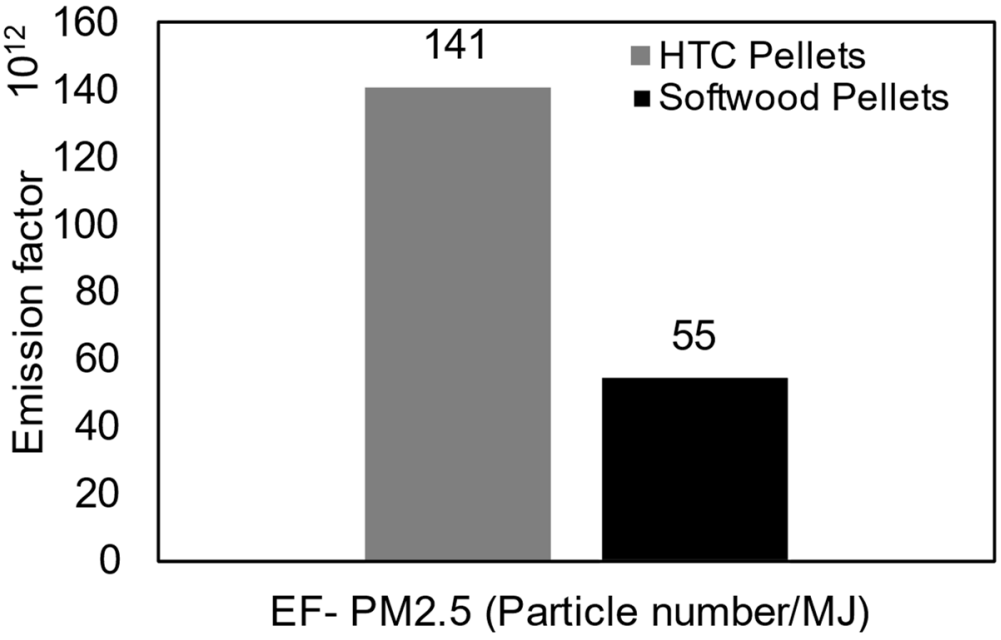

Figure 9. Emissions factor of softwood and HTC pellets for $PM_{2.5}$.

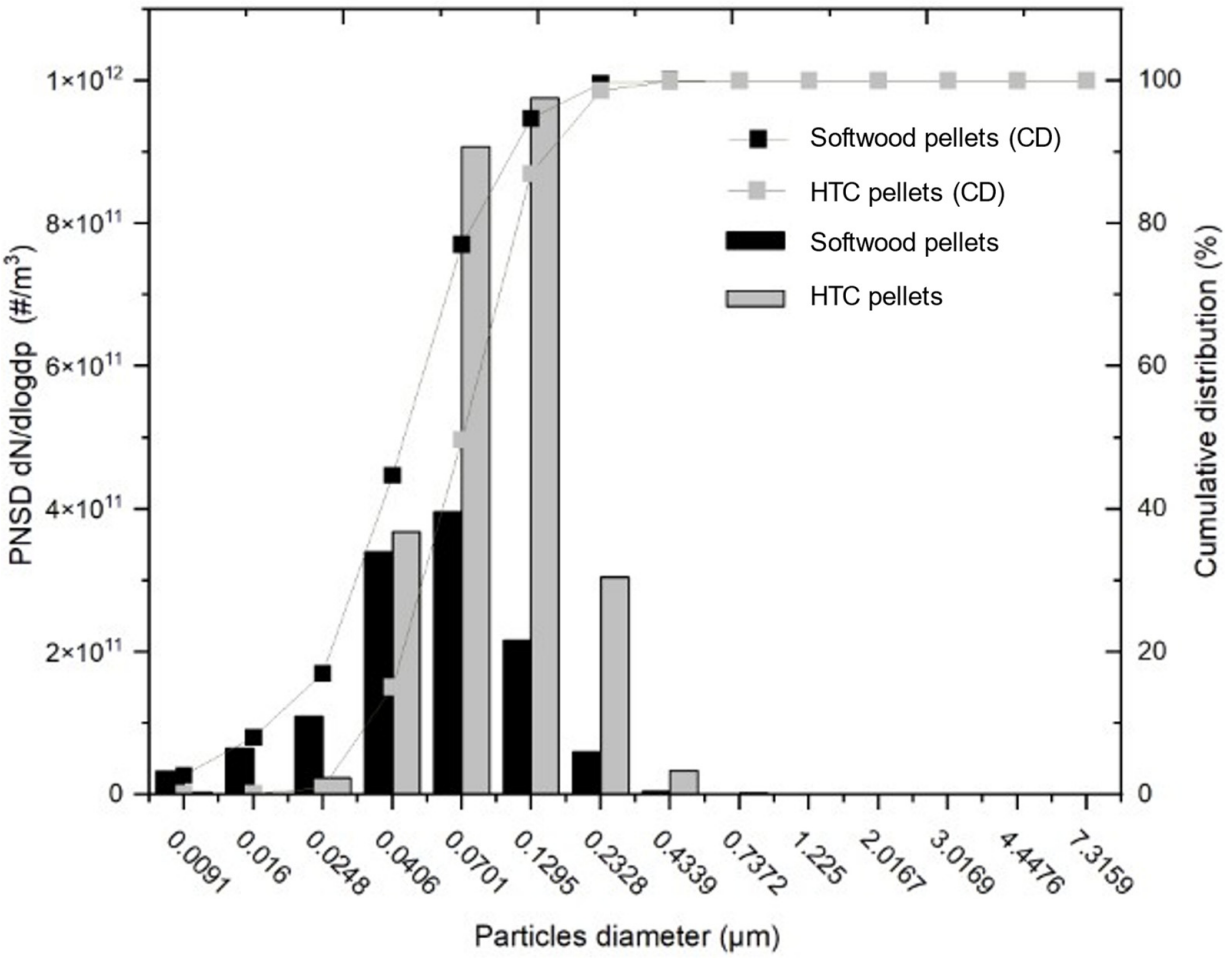

Figure 10. Particle number distribution and distribution of cumulative particle diameter. PNSD: particle number size distribution, and CD: cumulative distribution.

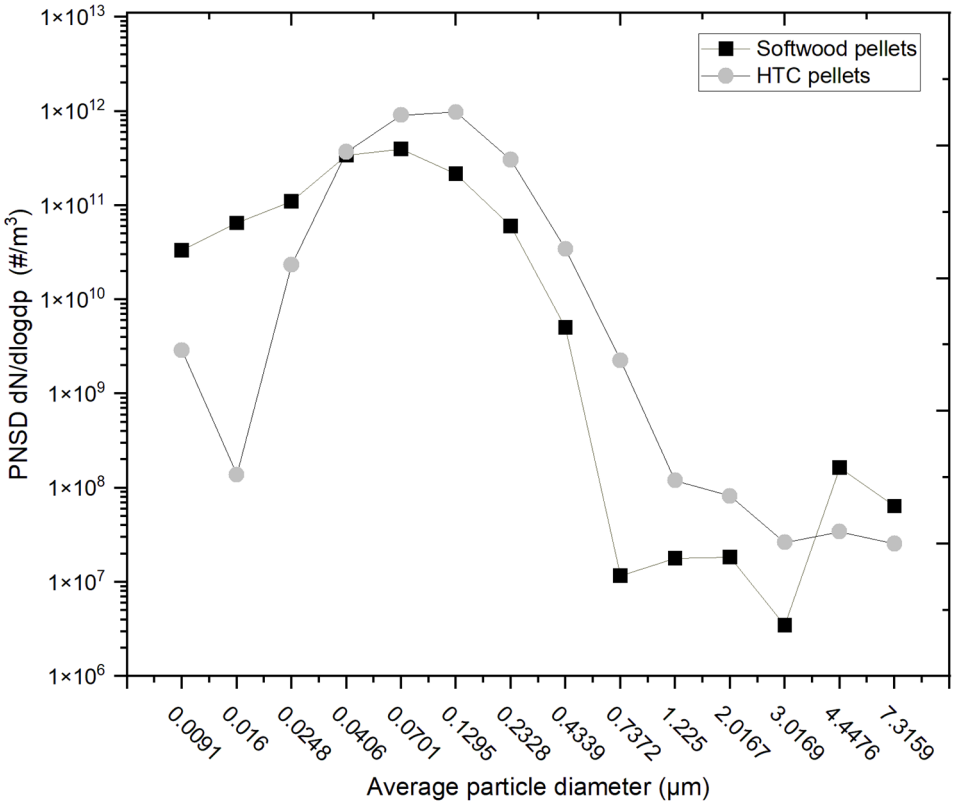

Figure 11. Particle-number size distribution (PNSD) versus average particle's diameter in logarithm coordinate.

Figure 11 shows how the particle number of softwood pellets is higher in the zone of smaller particle diameter and higher particle diameter than HTC pellets particle emission. Nevertheless, the total particle number emission was higher for the HTC pellets than for the softwood pellets. Han et al. [19] observed a trend in which the formation of vaporized matter decreases in torrefied fuels during combustion, typically resulting in a higher quantity of larger particles. The HTC process facilitates the reduction of chlorine and sulfur in its carbonized product. This will increase the presence of inorganic ash compounds (Na, Ca, Mg, and K) in less reactive forms, such as aluminosilicates in bottom and fly ashes. The elevated particle number in the smaller size range for softwood pellets aligns with these findings. However, a higher particle number for softwood pellets is evident for diameters of 4.8 µm and 7.3 µm. This is attributed to the lower combustion efficiency depicted in Figure 6 and the unburnt material illustrated in Figure 8 for softwood pellets, which may suggest the existence of larger unburnt carbon particles in the exhaust gases.

5. Conclusions

In this study, a comparison was made between the combustion kinetics, efficiencies, and pollutant emissions of green waste HTC pellets and softwood pellets.

Both pellet types exhibited two distinct peaks corresponding to combustion zones I and II in the DTG graphs Figures 2a and 3a). However, the HTC pellets showed a lower burning rate in zone I due to their lower volatile matter content. In zone III, a small amount of char required higher activation energy for its complete conversion, resulting in a very low reaction rate. This third reaction rate peak is associated with the fuel composition in terms of the high fixed carbon and ash content.

The combustion tests of HTC and softwood pellets have shown that HTC pellets outperform softwood pellets in terms of boiler efficiency and combustion efficiency. However, HTC pellets showed higher CO, NO_x, and $PM_{2.5}$ emission factors than the softwood pellets

in the tested operation mode. The PM emission results showed that most particles emitted are concentrated up to $PM_{2.5}$.

The mitigation of such emissions could be considered, to some extent, impractical for small boiler applications. However, implementing air-staging combustion could be an option to explore for reducing NO_x emissions, as well as partial recirculation of combustion products. On the other hand, air-staging combustion might increase CO emissions, and from a practical point of view, some physical modifications to the boiler may be required. The characteristic short residence time of combustion products in such small boilers seems to have a considerable impact on CO, NO_x, and PM emissions.

In general, the results suggest a good opportunity to optimize boiler operation in terms of the air-fuel ratio to minimize CO, NO_x, and PM emission factors, considering the advantages and disadvantages of tuning the air-fuel ratio parameter for boiler efficiency and emissions in a domestic heating application. The higher boiler efficiency during HTC pellet combustion compared to softwood pellet combustion presents an interesting opportunity to find a beneficial trade-off regarding thermal and environmental performance. Modifying boiler operational parameters, such as the fuel feeding rate or the amount of combustion air, could alter the combustion product residence time before exploring other alternatives, which might involve physical modifications.

Author Contributions: Y.G.L.: Conceptualization, Methodology, Investigation, Software, Visualization, Writing—Original Draft and Writing—Review & Editing; A.G.: Investigation, Data curation, Validation, and Writing—Review & Editing. L.G.: Investigation and Validation; J.B.: Methodology, Supervision, and Writing—Review & Editing; S.B.: Supervision, Methodology and Writing—Review & Editing. All authors have read and agreed to the published version of the manuscript.

Funding: This research received no external funding.

Data Availability Statement: Data is contained within the article.

Acknowledgments: This study was conducted with the support of the VUB University scholarship, funded by the VLIR-UOS program of the Flemish government, and with the support of the Cuban national project RAC-Bag with the code PN3602LH002.

Conflicts of Interest: The authors declare no conflicts of interest.

References

1. Lindberg, D.; Backman, R.; Chartrand, P.; Hupa, M. Towards a comprehensive thermodynamic database for ash-forming elements in biomass and waste combustion—Current situation and future developments. *Fuel Process. Technol.* **2013**, *105*, 129–141. [CrossRef]
2. Brigagão, G.V.; de Queiroz Fernandes Araújo, O.; de Medeiros, J.L.; Mikulcic, H.; Duic, N. A techno-economic analysis of thermochemical pathways for corncob-to-energy: Fast pyrolysis to bio-oil, gasification to methanol and combustion to electricity. *Fuel Process. Technol.* **2019**, *193*, 102–113. [CrossRef]
3. Li, Y.; Yang, X.; Zhu, M.; Dong, L.; Jiang, H.; Xu, Q.; Zhou, H.; Han, Y.; Feng, L.; Li, C. Synergistic effect of combined hydrothermal carbonization of Fenton's reagent and biomass enhances the adsorption and combustion characteristics of sludge towards eco-friendly and efficient sludge treatment. *Sci. Total Environ.* **2022**, *825*, 153854. [CrossRef]
4. Kassim, F.O.; Sohail, M.; Taylor, B.; Afolabi, O.O.D. Hydrothermal carbonisation of mixed agri-food waste: Process optimisation and mechanistic evaluation of hydrochar inorganic chemistry. *Biomass Bioenergy* **2024**, *180*, 107027. [CrossRef]
5. De Francesco, C.; Gasperini, T.; Duca, D.; Toscano, G.; Ilari, A. Hydrothermal Carbonization of Residual Biomass from Agricultural and Agro-Industrial Sector. *Processes* **2024**, *12*, 1673. [CrossRef]
6. Balmuk, G.; Cay, H.; Duman, G.; Kantarli, I.C.; Yanik, J. Hydrothermal carbonization of olive oil industry waste into solid fuel: Fuel characteristics and combustion performance. *Energy* **2023**, *278*, 127803. [CrossRef]
7. Prus, Z.; Wilk, M. Microplastics in Sewage Sludge: Worldwide Presence in Biosolids, Environmental Impact, Identification Methods and Possible Routes of Degradation, Including the Hydrothermal Carbonization Process. *Energies* **2024**, *17*, 4219. [CrossRef]
8. Koppejan, J.; Van Loo, S. *The Handbook of Biomass Combustion and Co-Firing*; Routledge: London, UK, 2012. [CrossRef]
9. Sitek, T.; Pospíšil, J.; Poláčik, J.; Chýlek, R. Thermogravimetric analysis of solid biomass fuels and corresponding emission of fine particles. *Energy* **2021**, *237*, 121609. [CrossRef]
10. Lasek, J.A.; Matuszek, K.; Hrycko, P.; Głód, K.; Li, Y.-H. The combustion of torrefied biomass in commercial-scale domestic boilers. *Renew. Energy* **2023**, *216*, 119065. [CrossRef]

11. Murillo, H.A.; Díaz-Robles, L.A.; Santander, R.E.; Cubillos, F.A. Conversion of residual oat husk and pine sawdust by co-hydrothermal carbonization towards biofuel production for pellet stoves. *Ind. Crops Prod.* **2021**, *174*, 114219. [CrossRef]
12. Ugolini, M.; Recchia, L.; Wray, H.E.; Dijkstra, J.W.; Nanou, P. Environmental Assessment of Hydrothermal Treatment of Wet Bio-Residues from Forest-Based and Agro-Industries into Intermediate Bioenergy Carriers. *Energies* **2024**, *17*, 560. [CrossRef]
13. Wu, S.; Wang, Q.; Fang, M.; Wu, D.; Cui, D.; Pan, S.; Bai, J.; Xu, F.; Wang, Z. Hydrothermal carbonization of food waste for sustainable biofuel production: Advancements, challenges, and future prospects. *Sci. Total Environ.* **2023**, *897*, 165327. [CrossRef]
14. Zhu, G.; Yang, L.; Gao, Y.; Xu, J.; Chen, H.; Zhu, Y.; Wang, Y.; Liao, C.; Lu, C.; Zhu, C. Characterization and pelletization of cotton stalk hydrochar from HTC and combustion kinetics of hydrochar pellets by TGA. *Fuel* **2019**, *244*, 479–491. [CrossRef]
15. Liang, M.; Lu, W.; Lei, P.; Wang, L.; Wang, B.; Li, B.; Shen, Y.; Zhang, K. Physical and Combustion Properties of Binder-Assisted Hydrochar Pellets from Hydrothermal Carbonization of Tobacco Stem. *Waste Biomass Valorization* **2020**, *11*, 6369–6382. [CrossRef]
16. Sharma, H.B.; Dubey, B.K. Binderless fuel pellets from hydrothermal carbonization of municipal yard waste: Effect of severity factor on the hydrochar pellets properties. *J. Clean. Prod.* **2020**, *277*, 124295. [CrossRef]
17. Moreira, B.R.d.A.; Cruz, V.H.; Pérez, J.F.; Viana, R.d.S. Production of pellets for combustion and physisorption of CO2 from hydrothermal carbonization of food waste—Part I: High-performance solid biofuels. *J. Clean. Prod.* **2021**, *319*, 128695. [CrossRef]
18. Namkung, H.; Park, J.-H.; Lee, Y.-J.; Song, G.-S.; Choi, J.W.; Park, S.-J.; Kim, S.; Liu, J.; Choi, Y.-C. Performance evaluation of biomass pretreated by demineralization and torrefaction for ash deposition and PM emissions in the combustion experiments. *Fuel* **2021**, *292*, 120379. [CrossRef]
19. Hansen, L.J.; Fendt, S.; Spliethoff, H. Impact of hydrothermal carbonization on combustion properties of residual biomass. *Biomass Convers. Biorefinery* **2022**, *12*, 2541–2552. [CrossRef]
20. Moloeznik Paniagua, D.; Libra, J.A.; Rotter, V.S.; Ro, K.S.; Fischer, M.; Linden, J. Enhancing Fuel Properties of Napier Grass via Carbonization: A Comparison of Vapothermal and Hydrothermal Carbonization Treatments. *Agronomy* **2023**, *13*, 2881. [CrossRef]
21. Saha, S.; Islam, M.T.; Calhoun, J.; Reza, T. Effect of Hydrothermal Carbonization on Fuel and Combustion Properties of Shrimp Shell Waste. *Energies* **2023**, *16*, 5534. [CrossRef]
22. Wang, G.; Li, R.; Dan, J.; Yuan, X.; Shao, J.; Liu, J.; Xu, K.; Li, T.; Ning, X.; Wang, C. Preparation of Biomass Hydrochar and Application Analysis of Blast Furnace Injection. *Energies* **2023**, *16*, 1216. [CrossRef]
23. Wu, S.; Wang, Q.; Cui, D.; Sun, H.; Yin, H.; Xu, F.; Wang, Z. Evaluation of fuel properties and combustion behaviour of hydrochar derived from hydrothermal carbonisation of agricultural wastes. *J. Energy Inst.* **2023**, *108*, 101209. [CrossRef]
24. Guo, S.; Deng, X.; Liu, L.; Ge, L.; Lisak, G. Comprehensive analysis of combustion behavior, kinetics, and gas emissions of fungus bran biofuel through torrefaction pretreatment and polypropylene addition. *Fuel* **2024**, *364*, 131014. [CrossRef]
25. Tamires da Silva Carvalho, N.; Silveira, E.A.; de Paula Protásio, T.; Trugilho, P.F.; Bianchi, M.L. Hydrotreatment of Eucalyptus sawdust: The influence of process temperature and H2SO4 catalyst on hydrochar quality, combustion behavior and related emissions. *Fuel* **2024**, *360*, 130643. [CrossRef]
26. Garcia Lovella, Y.; Goel, A.; Garin, L.; Blondeau, J.; Bram, S. Experimental Assessment of Green Waste HTC Pellets: Kinetics, Efficiency and Emissions. In Proceedings of the 36th International Conference on Efficiency, Cost, Optimization, Simulation and Environmental Impact of Energy Systems (ECOS 2023), Las Palmas, Spain, 25–30 June 2023; pp. 965–976.
27. Cornette, J.F.P.; Coppieters, T.; Lepaumier, H.; Blondeau, J.; Bram, S. Particulate matter emission reduction in small- and medium-scale biomass boilers equipped with flue gas condensers: Field measurements. *Biomass Bioenergy* **2021**, *148*, 106056. [CrossRef]
28. *ISO 17828*; Solid Biofuels—Determination of Bulk Density. ISO: Geneva, Switzerland, 2015.
29. *ISO 18134*; Solid Biofuels—Determination of Moisture Content—Oven Dry Method—Part 1: Total Moisture—Reference Method. ISO: Geneva, Switzerland, 2015.
30. *ISO 18122*; Solid Biofuels—Determination of Ash Content. ISO: Geneva, Switzerland, 2015.
31. *ISO 18123*; Solid Biofuels—Determination of Volatile Matter. ISO: Geneva, Switzerland, 2015.
32. *ISO 18125*; Solid Biofuels—Determination of Calorific Value. ISO: Geneva, Switzerland, 2015.
33. *ISO 16948*; Solid Biofuels—Determination of Total Content of Carbon, Hydrogen and Nitrogen. ISO: Geneva, Switzerland, 2015.
34. *ISO 16994*; Solid Biofuels—Determination of Total Content of Sulfur and Chlorine. ISO: Geneva, Switzerland, 2015.
35. TNO E. Phyllis2, Database for (Treated) Biomass, Algae, Feedstocks for Biogas Production and Biochar. Von Phyllis2, Database for (Treated) Biomass, Algae, Feedstocks for Biogas. 2020. Available online: https://phyllis.nl/ (accessed on 5 May 2023).
36. ENGIE-Laborelec. *Solid Biofuel Analysis*; Biomass Lab of Laborelec: Brussels, Belgium, 2022; p. 3.
37. Mason, D.M.; Gandhi, K.N. Formulas for calculating the calorific value of coal and coal chars: Development, tests, and uses. *Fuel Process. Technol.* **1983**, *7*, 11–22. [CrossRef]
38. Cornette, J. Experimental and Numerical Assessment of Particle Size Distributions from Solid Biomass Combustion. Ph.D. Thesis, Mechanical Departament, Vrije Universiteit Brussels, Brussels, Belgium, 2022.
39. Liu, J.; Jiang, X.; Cai, H.; Gao, F. Study of Combustion Characteristics and Kinetics of Agriculture Briquette Using Thermogravimetric Analysis. *ACS Omega* **2021**, *6*, 15827–15833. [CrossRef]
40. Escalante, J.; Chen, W.-H.; Tabatabaei, M.; Hoang, A.T.; Kwon, E.E.; Andrew Lin, K.-Y.; Saravanakumar, A. Pyrolysis of lignocellulosic, algal, plastic, and other biomass wastes for biofuel production and circular bioeconomy: A review of thermogravimetric analysis (TGA) approach. *Renew. Sustain. Energy Rev.* **2022**, *169*, 112914. [CrossRef]

41. Lu, J.-J.; Chen, W.-H. Investigation on the ignition and burnout temperatures of bamboo and sugarcane bagasse by thermogravimetric analysis. *Appl. Energy* **2015**, *160*, 49–57. [CrossRef]
42. Rago, Y.P.; Collard, F.-X.; Görgens, J.F.; Surroop, D.; Mohee, R. Co-combustion of torrefied biomass-plastic waste blends with coal through TGA: Influence of synergistic behaviour. *Energy* **2022**, *239*, 121859. [CrossRef]
43. Moon, C.; Sung, Y.; Ahn, S.; Kim, T.; Choi, G.; Kim, D. Effect of blending ratio on combustion performance in blends of biomass and coals of different ranks. *Exp. Therm. Fluid Sci.* **2013**, *47*, 232–240. [CrossRef]
44. Hoang, A.T.; Ong, H.C.; Fattah, I.M.R.; Chong, C.T.; Cheng, C.K.; Sakthivel, R.; Ok, Y.S. Progress on the lignocellulosic biomass pyrolysis for biofuel production toward environmental sustainability. *Fuel Process. Technol.* **2021**, *223*, 106997. [CrossRef]
45. Bridgwater, A.V.; Meier, D.; Radlein, D. An overview of fast pyrolysis of biomass. *Org. Geochem.* **1999**, *30*, 1479–1493. [CrossRef]
46. Kissinger, H.E. Reaction Kinetics in Differential Thermal Analysis. *Anal. Chem.* **1957**, *29*, 1702–1706. [CrossRef]
47. Akahira, T.; Sunose, T. Method of determining activation deterioration constant of electrical insulating materials. *Res. Rep. Chiba Inst. Technol. (Sci. Technol.)* **1971**, *16*, 22–31.
48. Flynn, J.H.; Wall, L.A. A quick, direct method for the determination of activation energy from thermogravimetric data. *J. Polym. Sci. Part B Polym. Lett.* **1966**, *4*, 323–328. [CrossRef]
49. Ozawa, T. A new method of analyzing thermogravimetric data. *Bull. Chem. Soc. Jpn.* **1965**, *38*, 1881–1886. [CrossRef]
50. Coats, A.W.; Redfern, J.P. Kinetic Parameters from Thermogravimetric Data. *Nature* **1964**, *201*, 68–69. [CrossRef]
51. Nussbaumer, T.; Good, J. Determination of the combustion efficiency in biomass furnaces. In Proceedings of the 10th European Conference and Technology Exhibition Biomass for Energy, Industry and Climate Protection, Würzburg, Germany, 8–11 June 1998.
52. Good, J.; Nussbaumer, T. Wirkungsgradbestimmung bei Holzfeuerungen. Bezugsquelle: Zürich, Switzerland, 1993.
53. Good, J.; Nussbaumer, T.; Delcarte, J.; Schenkel, Y. Determination of the Efficiencies of Automatic Biomass Combustion Plants. Verenum International Energy Agency, IEA Bioenergy Task; IEA: Paris, France, 2006; Volume 32.
54. Lyubov, V.K.; Malygin, P.V.; Popov, A.N.; Popova, E.I. Determining heat loss into the environment based on comprehensive investigation of boiler performance characteristics. *Therm. Eng.* **2015**, *62*, 572–576. [CrossRef]
55. Gil, M.V.; Oulego, P.; Casal, M.D.; Pevida, C.; Pis, J.J.; Rubiera, F. Mechanical durability and combustion characteristics of pellets from biomass blends. *Bioresour. Technol.* **2010**, *101*, 8859–8867. [CrossRef]
56. Jiang, L.; Yuan, X.; Xiao, Z.; Liang, J.; Li, H.; Cao, L.; Wang, H.; Chen, X.; Zeng, G. A comparative study of biomass pellet and biomass-sludge mixed pellet: Energy input and pellet properties. *Energy Convers. Manag.* **2016**, *126*, 509–515. [CrossRef]
57. Jia, G. Combustion characteristics and kinetic analysis of biomass pellet fuel using thermogravimetric analysis. *Processes* **2021**, *9*, 868. [CrossRef]
58. Chen, D.; Gao, A.; Cen, K.; Zhang, J.; Cao, X.; Ma, Z. Investigation of biomass torrefaction based on three major components: Hemicellulose, cellulose, and lignin. *Energy Convers. Manag.* **2018**, *169*, 228–237. [CrossRef]
59. Khoo, C.G.; Lam, M.K.; Mohamed, A.R.; Lee, K.T. Hydrochar production from high-ash low-lipid microalgal biomass via hydrothermal carbonization: Effects of operational parameters and products characterization. *Environ. Res.* **2020**, *188*, 109828. [CrossRef]
60. Mancarella, F.; D'Elia, M.; Micca Longo, G.; Longo, S.; Orofino, V. Kinetics of Thermal Decomposition of Particulate Samples of MgCO3: Experiments and Models. *Chemistry* **2022**, *4*, 548–559. [CrossRef]
61. Zheng, J.; Huang, J.; Tao, L.; Li, Z.; Wang, Q. A Multifaceted Kinetic Model for the Thermal Decomposition of Calcium Carbonate. *Crystals* **2020**, *10*, 849. [CrossRef]
62. Ozgen, S.; Cernuschi, S.; Caserini, S. An overview of nitrogen oxides emissions from biomass combustion for domestic heat production. *Renew. Sustain. Energy Rev.* **2021**, *135*, 110113. [CrossRef]
63. Vakkilainen, E.K. 2—Solid Biofuels and Combustion. In *Steam Generation from Biomass*; Vakkilainen, E.K., Ed.; Butterworth-Heinemann: Oxford, UK, 2017; pp. 18–56. [CrossRef]
64. Speth, K.; Murer, M.; Spliethoff, H. Experimental Investigation of Nitrogen Species Distribution in Wood Combustion and Their Influence on NOx Reduction by Combining Air Staging and Ammonia Injection. *Energy Fuels* **2016**, *30*, 5816–5824. [CrossRef]
65. Liu, X.; Luo, Z.; Yu, C. Conversion of char-N into NO_x and N_2O during combustion of biomass char. *Fuel* **2019**, *242*, 389–397. [CrossRef]
66. Zhou, H.; Li, Y.; Li, N.; Qiu, R.; Meng, S.; Cen, K. Experimental study of the NO and N_2O emissions during devolatilization and char combustion of a single biomass particle in O2/N2 and O2/H2O under low temperature condition. *Fuel* **2017**, *206*, 162–170. [CrossRef]
67. Kaivosoja, T.; Jalava, P.I.; Lamberg, H.; Virén, A.; Tapanainen, M.; Torvela, T.; Tapper, U.; Sippula, O.; Tissari, J.; Hillamo, R.; et al. Comparison of emissions and toxicological properties of fine particles from wood and oil boilers in small (20–25 kW) and medium (5–10 MW) scale. *Atmos. Environ.* **2013**, *77*, 193–201. [CrossRef]